

Supplement of Atmos. Chem. Phys., 18, 15921–15935, 2018
<https://doi.org/10.5194/acp-18-15921-2018-supplement>
© Author(s) 2018. This work is distributed under
the Creative Commons Attribution 4.0 License.



Supplement of

Relationships between the planetary boundary layer height and surface pollutants derived from lidar observations over China: regional pattern and influencing factors

Tianning Su et al.

Correspondence to: Zhanqing Li (zli@atmos.umd.edu)

The copyright of individual parts of the supplement might differ from the CC BY 4.0 License.

24 **Table S1.** Mean values and standard deviation (STD) of CALIPSO-PBLH, MERRA-PBLH, and PM_{2.5}

25 over different ROIs.

| Parameter | | | NCP | PRD | YRD | NEC | |
|---|--------------------|------|-------|------|------|------|------|
| CALIPSO-PBLH (km) | MAM | Mean | 1.40 | 1.35 | 1.31 | 1.40 | |
| | | STD | 0.54 | 0.47 | 0.48 | 0.59 | |
| | JJA | Mean | 1.47 | 1.27 | 1.24 | 1.46 | |
| | | STD | 0.51 | 0.44 | 0.46 | 0.55 | |
| | SON | Mean | 1.21 | 1.24 | 1.26 | 1.15 | |
| | | STD | 0.45 | 0.36 | 0.39 | 0.50 | |
| | DJF | Mean | 1.06 | 1.07 | 1.12 | 0.94 | |
| | | STD | 0.40 | 0.34 | 0.41 | 0.47 | |
| | MERRA-PBLH (km) | MAM | Mean | 1.57 | 1.16 | 1.24 | 1.45 |
| | | | STD | 0.75 | 0.53 | 0.47 | 0.69 |
| JJA | | Mean | 1.46 | 0.99 | 1.07 | 1.49 | |
| | | STD | 0.72 | 0.36 | 0.39 | 0.68 | |
| SON | | Mean | 1.37 | 1.18 | 1.22 | 1.19 | |
| | | STD | 0.48 | 0.37 | 0.33 | 0.54 | |
| DJF | | Mean | 1.08 | 1.09 | 1.05 | 0.65 | |
| | | STD | 0.36 | 0.40 | 0.32 | 0.36 | |
| PM _{2.5} ($\mu\text{g m}^{-3}$) | | MAM | Mean | 63.1 | 32.8 | 50.4 | 34.8 |
| | | | STD | 45.1 | 22.1 | 29.2 | 29.4 |
| | JJA | Mean | 51.2 | 25.1 | 37.9 | 29.6 | |
| | | STD | 36.8 | 20.4 | 24.1 | 24.4 | |
| | SON | Mean | 70.9 | 39.3 | 42.4 | 44.2 | |
| | | STD | 58.4 | 23.1 | 28.3 | 49.1 | |
| | DJF | Mean | 102.7 | 44.2 | 69.8 | 60.3 | |
| | | STD | 84.2 | 28.3 | 51.3 | 54.4 | |

26

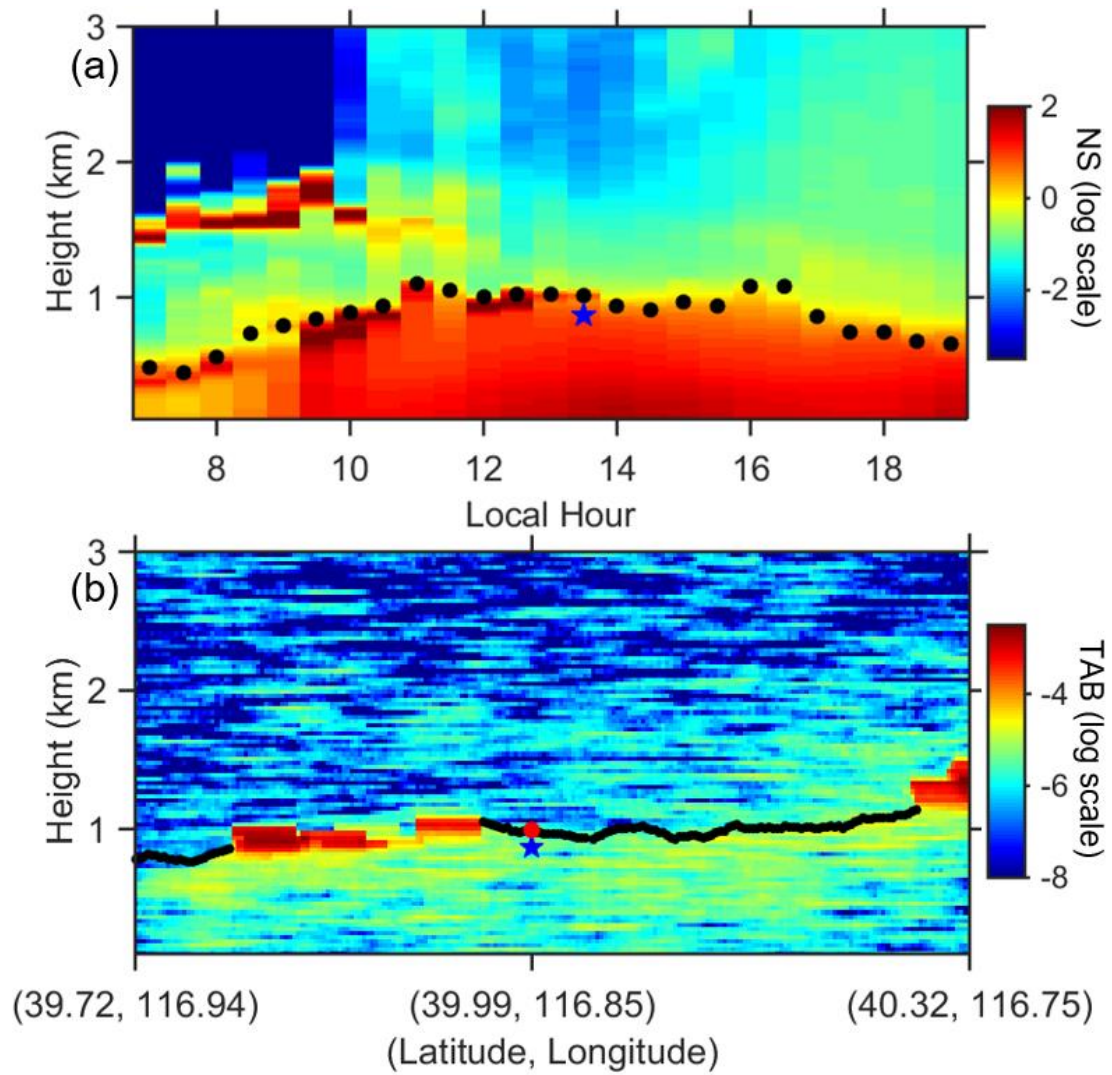


Figure S1. (a) Time evolution of the normalized signal (NS) plot from MPL on 7 June 2016 over Beijing. The black dots identify the PBLH derived from MPL, and the blue star indicates the PBLH derived from radiosonde. (b) Total attenuated backscatter (TAB) plot (log scale) from CALIPSO on 7 June 2016 over Beijing. The black line indicate the PBLH derived from CALIPSO. The red dot represents the corresponding PBLH derived from MPL, and the blue star indicates the PBLH derived from radiosonde.

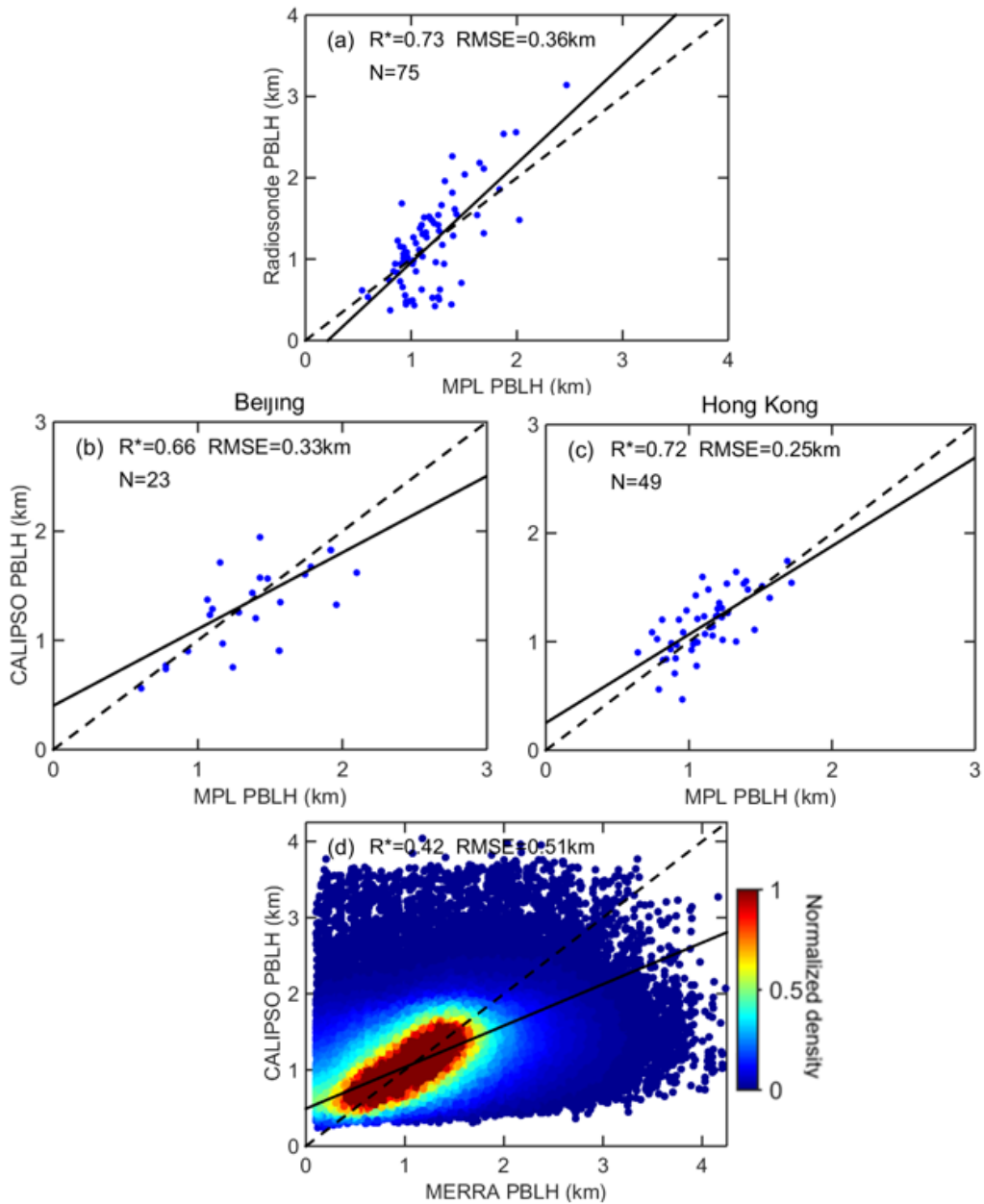


Figure S2. (a) Comparison of PBLHs derived from MPL and radiosonde at 1400 CST over Beijing. (b) Comparison of PBLHs derived from CALIPSO and MPL at Beijing. (c) Comparison of PBLHs derived from CALIPSO and MPL at Hong Kong. This comparison is adapted from Su et al. (2017). (d) Comparison of PBLHs derived from CALIPSO and MERRA. The correlation coefficients (R), RMSE, and number of samples (N) are given in each panel. (Note that the sample number in (d) is ~500000). R with asterisks indicates the correlation is statistically significant at the 99% confidence level.

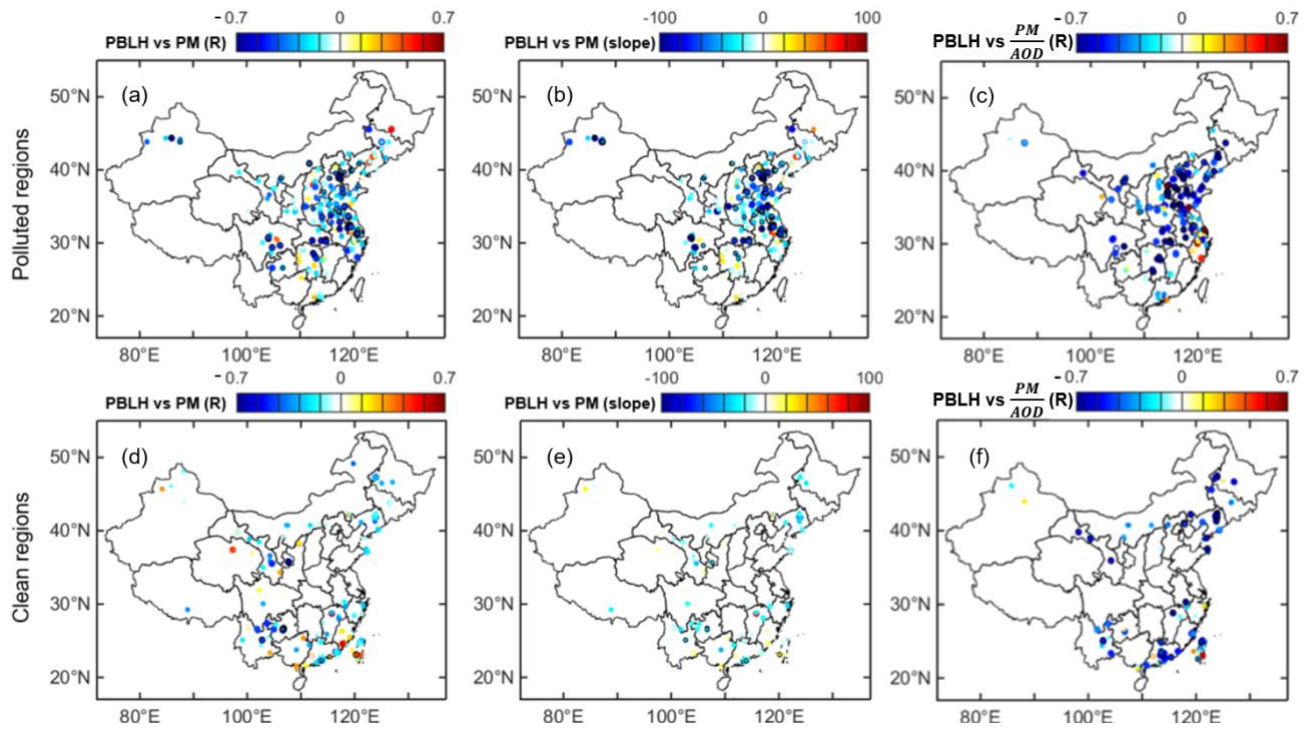


Figure S3. Stratification by annual pollution levels. The correlation coefficients (R) and slopes between PBLH and early-afternoon $PM_{2.5}$ derived from linear fitting for polluted regions (a-b) (annual mean $PM_{2.5} > 40 \mu g m^{-3}$) and clean regions (d-e) (annual mean $PM_{2.5} < 40 \mu g m^{-3}$). The correlation coefficients (R) between PBLH and $PM_{2.5}/AOD$ derived from linear fitting for polluted regions (c) and clean regions (f). Note that the PBLH-PM correlations are much stronger for polluted regions. After normalizing $PM_{2.5}$ by AOD, the correlations are stronger for most stations, especially for those over clean regions.

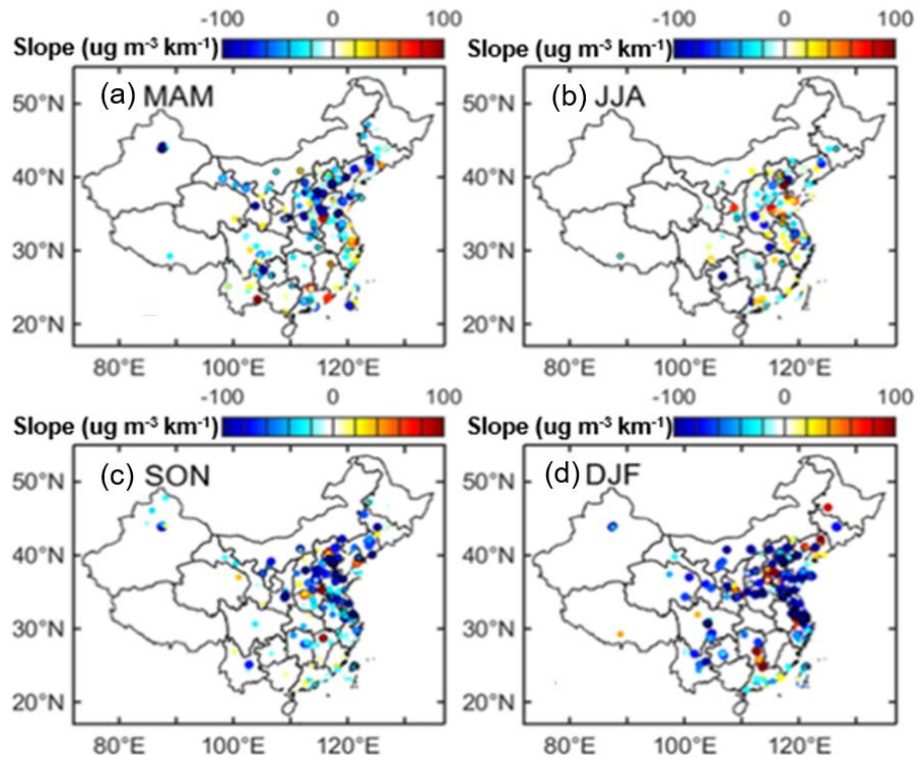


Figure S4. Spatial distributions of the PBLH-PM_{2.5} relationship slopes derived from the linear fitting for (a) MAM, (b) JJA, (c) SON, and (d) DJF.

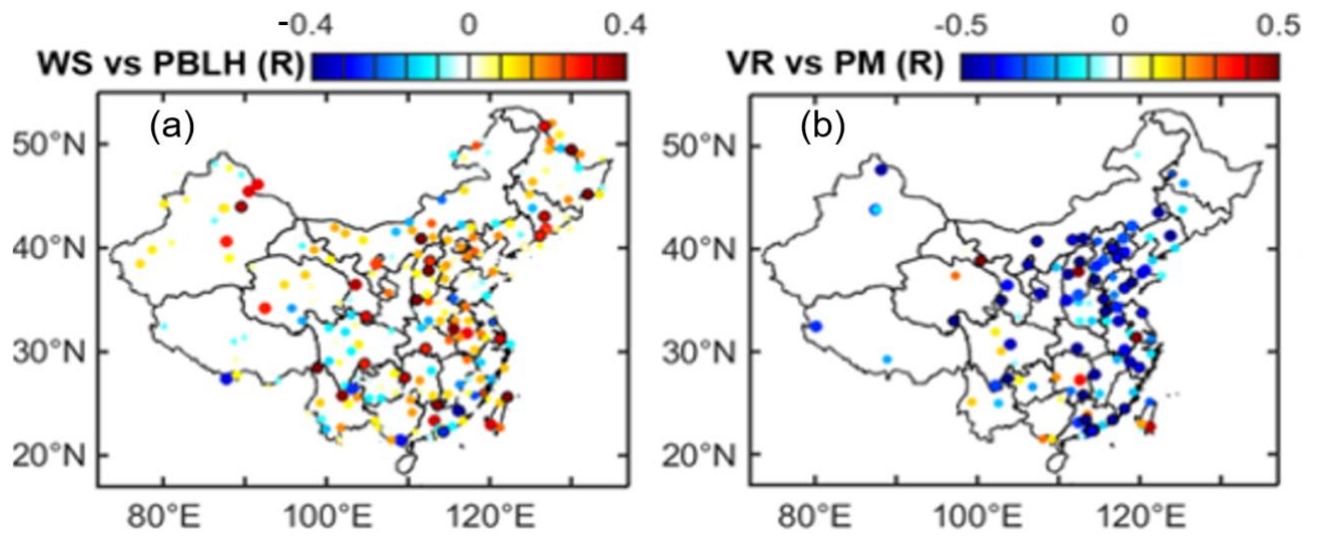


Figure S5. (a) Spatial distribution of linear correlation coefficients (R) for the WS-PBLH relationship. (b) Spatial distribution of correlation coefficients (R) for the VR-PM_{2.5} relationship.

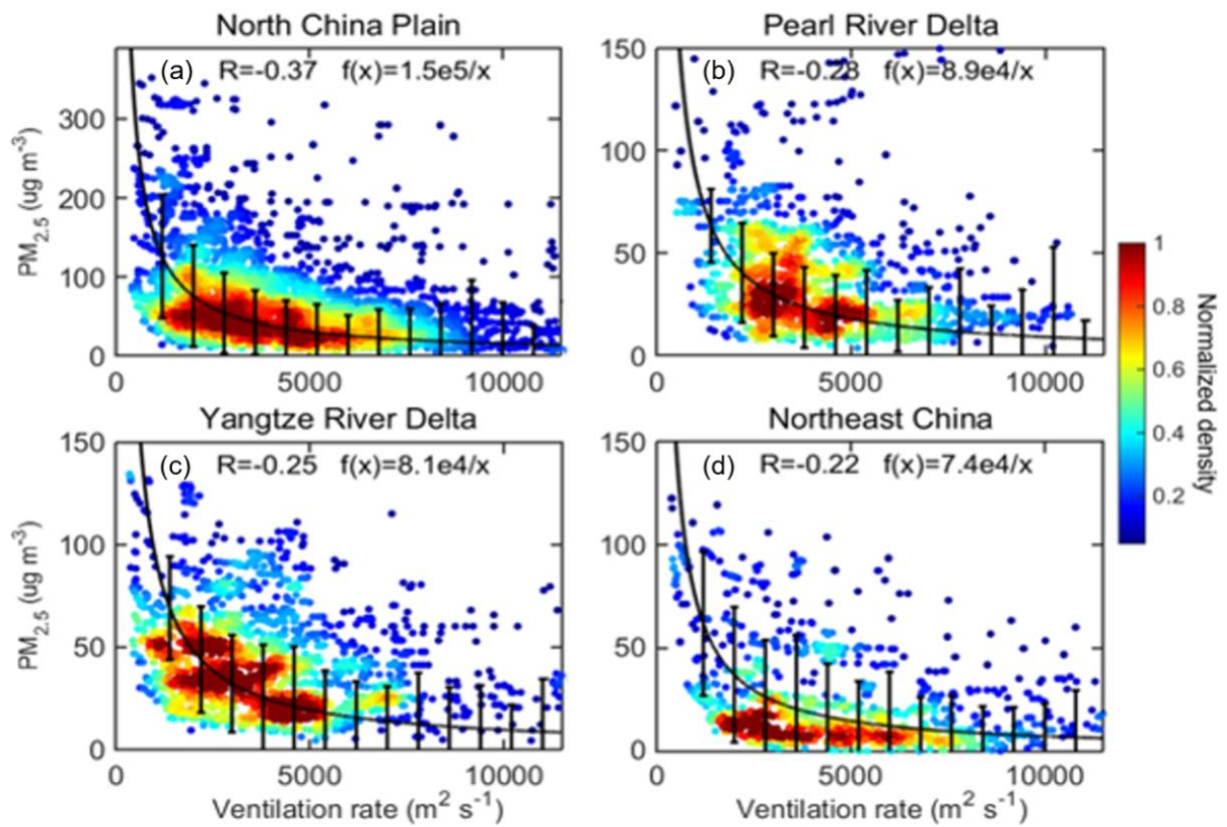


Figure S6. The relationship between early-afternoon $PM_{2.5}$ and ventilation rate over (a) the NCP, (b) PRD, (c) YRD, and (d) NEC.

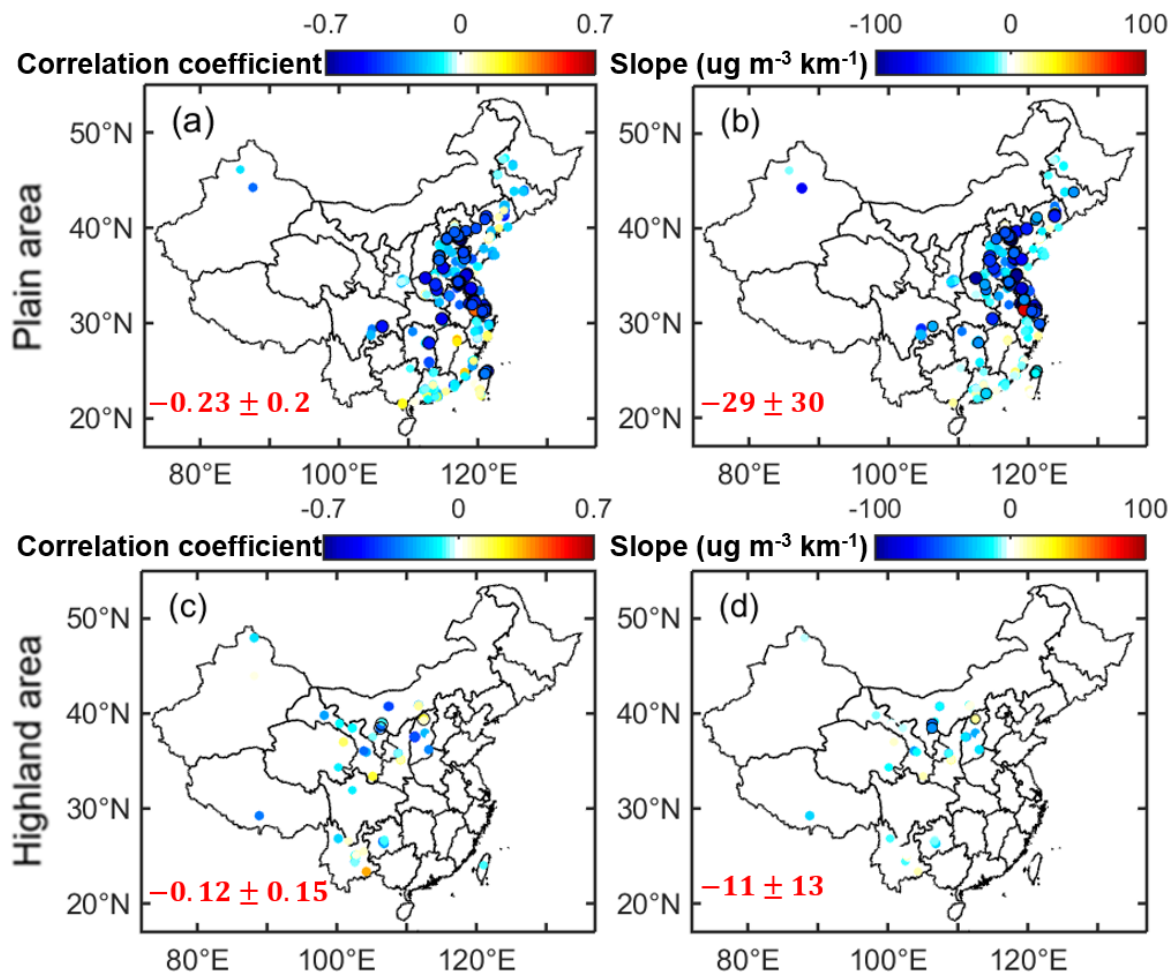


Figure S7. Similar to Figure 12a-d, but for the correlation coefficients and slopes of PBLH-PM relationships derived from the linear method. In the main text, we use the inverse fitting method to reveal the different PBLH-PM relationships between plains and highland areas, and we can find similar conclusions using the linear fitting method.

References

Su, T., Li, J., Li, C., Xiang, P., Lau, A.K.H., Guo, J., Yang, D. and Miao, Y.: An inter-comparison of long-term planetary boundary layer heights retrieved from CALIPSO, ground-based lidar, and radiosonde measurements over Hong Kong. *Journal of Geophysical Research: Atmospheres*, 122(7), pp.3929-3943, 2017.